



# BEMD BASED CROSS BILATERAL FILTERING TECHNIQUE FOR SPECKLE REDUCTION IN ULTRASOUND IMAGES

Bhawna GUPTA , Vineet KHANDELWAL 

Department of Electronics and Communication Engineering, Jaypee Institute of Information Technology, Sector-62, 201309 Noida, Uttar Pradesh, India

bhawna.gupta@jiit.ac.in, vineet.khandelwal@jiit.ac.in

DOI: 10.15598/aeec.v20i1.4265

Article history: Received Jun 22, 2021; Revised Nov 22, 2021; Accepted Dec 28, 2021; Published Mar 31, 2022.  
This is an open access article under the BY-CC license.

**Abstract.** In this paper, Bidimensional Empirical Mode Decomposition (BEMD) based Cross Bilateral Filter (CBF) technique for speckle reduction in ultrasound images has been proposed. The reference image is obtained by denoising the noisy image using pixel-wise Wiener filtering. Then, both the noisy image and the reference image are decomposed into a set of Intrinsic Mode Functions (IMFs) and the residue image using BEMD technique. CBF is applied between noisy image IMFs and the corresponding reference image IMFs. The image is reconstructed back with these modified IMFs and the residue. The proposed method exploits the edge information in the reference image for improving the quality of the denoised image. The performance of the proposed method has been tested for real ultrasound images and simulated images having noise of different variance. The experimental results show that the proposed algorithm performs better than other state-of-art methods in terms of Edge Keeping Index (EKI), Correlation Coefficient (CC), Figure of Merit (FOM), Structural Similarity (SSIM), Peak Signal to Noise Ratio (PSNR) and Signal to Noise Ratio (SNR) for synthetic images. The algorithm gives better performance for real ultrasound images in terms of Mean to Variance Ratio (MVR) and Equivalent Number of Looks (ENL).

## Keywords

**BEMD, CBF, noise reduction, speckle.**

## 1. Introduction

With the advancement of various image acquiring hardware in applications like medical diagnosis, synthetic aperture radars, or aviation, large number of images are being acquired and utilized. These digital images available in large magnitude are affected by noise due to various external as well as internal factors. One such widely used application for diagnostic purposes is ultrasound image, whose perceived quality is degraded by the existence of speckle noise which is imminent owing to the presence of physical phenomenon such as scattering at the time of image acquisition [1]. Due to the high frequency characteristic of speckle noise, denoising algorithms utilized to improve the quality of these images face the challenge of preserving the edge information. Speckle reduction in ultrasound images is an essential step and targets improvement in the quality of the image in terms of PSNR, CC, SNR, FOM, SSIM, EKI, MVR and ENL [2], [3] and [4].

The state-of-the-art speckle reduction algorithms work in spatial domain. The spatial domain techniques mainly use local statistics or information redundancy between similar patches and replace the pixel value by processing the nearby pixel values. Most successful amongst this category are diffusion-based filters like Speckle Reducing Anisotropic Diffusion (SRAD), Detail preserving anisotropic diffusion (DPAD), Perona-Malik's Anisotropic Diffusion (PMAD) [5], [6], [7] and [8], Bilateral filters [9] and [10], and patch-based methods like Non Local Mean Filter (NLM) [11], [12], [13] and [14] and Optimized Bayesian Nonlocal Mean filter (OBNLM) [15] and [16]. The patch selection in patch-based methods is tricky so that the noise removal does not lose the edge information while denoising. Therefore, recent works [17], [18] and [19] use

modified NLM and Block Matching and 3D filtering (BM3D) algorithms to reduce speckle while trying to preserve the edge information.

Amongst these various methods, the bilateral filter proposed by Tomasi and Manduchi in 1998 [9] aims to denoise the image while preserving edge details by weight averaging the neighboring pixels based on their spatial distance and similarity. It has been applied to various fields like image denoising [9] and [20], photograph enhancement [21], or range compression [22], as it is non-iterative, simple and delivers a stable performance comparable to many other filters. The disadvantage of long running time of this method has been worked upon by various methods [22], [23] and [24]. Bilateral filtering has also been applied in wavelet domain for denoising in [20], which represents interesting results but does not perform well for real image denoising. In severe noise cases, the performance of non-local methods is better but that is at the cost of computation complexity and limitation of over smoothing the image. High quality denoised image by local processing can be obtained by joint bilateral filter [21] and [25], which calculates weights using another reference image. Getting high quality pre-estimated reference image is a crucial step in this method as the result depends on the chosen reference image.

Empirical Mode Decomposition (EMD) introduced in 1998 [26] is a very powerful algorithm decomposing the signal in its IMFs [27]. This decomposition is done based on their oscillation in the spatial domain. The basis functions calculated in this method are signal-dependent and a series of IMFs are estimated via an iterative procedure known as sifting [28]. The EMD was introduced in images in 2003 in [29] and the BEMD for images was introduced in 2005 in [30]. The BEMD is also a signal-dependent adaptive technique, decomposing the image into a series of IMFs and a residue. The low-order IMFs are the high-frequency components and the high order IMFs are the low-frequency components. The speckle noise has high frequency characteristic, therefore the low order IMFs are having more noise components as compared to the high order IMFs. Accordingly, some BEMD based denoising algorithms utilizes this fact to discard the noise existing in the low order IMFs [31], [32] and [33]. But this may not always be true and a significant noise component may also be present in further IMFs as well.

The CBF was introduced in 2004 to denoise low-light image [21] and to enhance the ambient image that rely on flash photograph information [25]. These methods are based on Bilateral filter equation and exploits the fact that the Signal to-Noise Ratio (SNR) of the flash image is higher than that of the no-flash image. Denoising algorithms can exploit this technique for images, where reference image is the one with higher SNR. As in most of the cases, the original noiseless image is not

available so choosing the correct reference image is a challenge. Laplacian pyramid has been utilized for denoising image using CBF in [34], where the reference image has been taken as the Wiener filtered version of the noisy image. Some other CBF based image denoising algorithms combine Non-local Means [35] and multi-sized 2D hard thresholding [36] for significant results. Most of the high-frequency components of the image contain detail information such as edges. Most of the noise is also in high frequency, therefore, these algorithms though giving good denoising performance, loose important edge details. These details are of importance for diagnostic purposes when dealing with ultrasound images.

This paper introduces a hybrid technique wherein the high SNR reference image is calculated using Wiener filtering the noisy image. The IMF's are computed for both noisy image and reference image. The edge information in the reference image IMFs is a crucial information that is important from the point of view of diagnosis. The proposed technique utilizes this edge information in reference image for obtaining a better quality denoised image in terms of edge details. To achieve this, a CBF is applied between the noisy image IMFs and the corresponding reference image IMFs to get despeckled image. This helps in preserving the edge information while denoising the ultrasound image.

The remainder of the paper is organized as follows. Section 2, provides a brief overview of BEMD algorithm along with CBF algorithm. In Sec. 3, the proposed denoising method is described. The performance evaluation of the proposed method is illustrated in Sec. 4, and Sec. 5 presents the conclusions.

## 2. Background

### 2.1. Bidimensional Empirical Mode Decomposition

BEMD is an adaptive technique which can be applied to images to decompose them into a set of various IMFs and a residue. The steps for calculation of the IMFs and the residue are as illustrated here.

Let the observed image be denoted by  $o(x, y)$ . This being an iterative process, let the residue of the  $m$ th IMF be represented by  $r_m(x, y)$ , which is taken as the input for the calculation of the next IMF. Let the input image taken for the generation of  $m$ th number IMF,  $m = 1, \dots, M$  at the  $k$ th iteration of the sifting process,  $k = 0, \dots, K - 1$  in two spatial dimensions  $(x, y)$ , be denoted by  $i_{m,k}(x, y)$ .

1. Initializing the sifting process for the calculation of the first IMF with  $m = 1$  and  $k = 0$ ,  $i_{m,k}(x, y)$

is taken to be the observed image. i.e  $i_{1,0}(x, y) = o(x, y)$ .

2. Local maxima and minima of  $i_{m,k}(x, y)$  are extracted.
3. Using the application specific spline interpolation for all local maxima, calculate the upper envelope  $u_e(x, y)$ . Also, using the interpolation of all local minima, calculate the lower envelope  $l_e(x, y)$ .
4. The mean envelope  $\overline{env}_{m,k}(x, y)$  is calculated from the upper and lower envelopes obtained in step 3.

$$\overline{env}_{m,k}(x, y) = \frac{u_e(x, y) + l_e(x, y)}{2}. \quad (1)$$

5. The mean envelope  $\overline{env}_{m,k}(x, y)$  is subtracted from the input signal for calculating the updated signal for the next iteration.

$$i_{m,k}(x, y) = i_{m,k-1}(x, y) - \overline{env}_{m,k}(x, y), \quad (2)$$

$k \rightarrow k + 1.$

6. Calculate the standard deviation  $\varepsilon$ , from the result obtained in step 5.

$$\varepsilon = \sum_{x=0}^{M-1} \sum_{y=0}^{N-1} \frac{|i_{m,k}(x, y) - i_{m,k-1}(x, y)|^2}{i_{m,k-1}^2(x, y)}. \quad (3)$$

7. If the standard deviation  $\varepsilon$  calculated in step 6 is less than a predefined value (usually 0.2–0.3), then the result of step 5 is the required  $m$ th IMF  $o_m(x, y)$ , else repeat steps 2–6.

$$o_m(x, y) = i_{m,k}(x, y). \quad (4)$$

8. The residue of the  $m$ th IMF is defined as:

$$r_m(x, y) = i_{m,0}(x, y) - o_m(x, y). \quad (5)$$

9. For the calculation of the next IMF this residue calculated in step 8 is taken as the input signal and going back to step 2 again.

$$i_{m+1,0}(x, y) = r_m(x, y). \quad (6)$$

Steps 2–9 are repeated until residue calculated has no more extrema points. Thus, for total of ‘M’ IMFs and the last residue  $r_M$ , the original signal can be represented as:

$$o(x, y) = \sum_{m=1}^M i_m(x, y) + r_M(x, y). \quad (7)$$

The high order IMFs are corresponding to the low frequency while low order IMFs, are corresponding to the high frequency.

## 2.2. Cross Bilateral Filter

CBF algorithm is explained here in brevity for the sake of illustration. Let  $I_n$  and  $I_r$  denote the noisy image and the reference image, respectively. The function  $g_d$  attenuates the filter kernel weights in spatial domain on the basis of the distance between the pixels. Also, the edge stopping function  $g_e$  sets weights on the basis of intensity difference between the pixels. Then the value of the pixel at location  $q$  using CBF can be calculated as:

$$I_q^{CBF} = \frac{1}{n(q)} \sum_{q' \in \Omega} g_d(\|q - q'\|) q_e(I_{rq} - I_{rq'}) I_{nq'}, \quad (8)$$

where  $n(q)$  is the normalization factor given by:

$$n_q = \sum_{q' \in \Omega} g_d(\|q - q'\|) q_e(I_{rq} - I_{rq'}), \quad (9)$$

and  $\Omega$  is the window size. The distance scaling function  $g_d$  is Gaussian function as given in Eq. (10), where standard deviation  $\sigma_d$  controls its width and the variable  $x$  in equation is Euclidean distance between  $q$  and  $q' \in \Omega$ .

$$g(x) = \exp\left(-\frac{x^2}{2\sigma_d^2}\right). \quad (10)$$

The edge stopping function  $g_e$  is also Gaussian function as given in Eq. (11) below where standard deviation  $\sigma_e$  is controlling its width.

$$g_e(I_{rq} - I_{rq'}) = \exp\left(-\frac{1}{2} \left(\frac{I_r(q) - I_r(q')}{\sigma_e}\right)^2\right). \quad (11)$$

The standard deviation  $\sigma_d$  is obtained as in conventional Bilateral filtering. Also, as the reference image has less noise,  $\sigma_e$  is not set very large. Even when the value of  $\sigma_e$  is taken small and fixed value of  $\sigma_e$  is taken for all images, the edge stopping function  $g_e$  ensures that proper weights are chosen without over-blurring or under-blurring the images.

## 3. BEMD Based Cross-Bilateral Filtering

This section introduces the proposed BEMD based cross bilateral filter for speckle reduction in Ultrasound images. The original image has speckle noise as well as the vital edge information in the high frequency components and this is reflected in the low order IMFs of the image. Reference image is obtained after processing the original image with Wiener filter. This reference image is being decomposed using BEMD algorithm to get a set of IMFs. Obtained low order IMFs retain

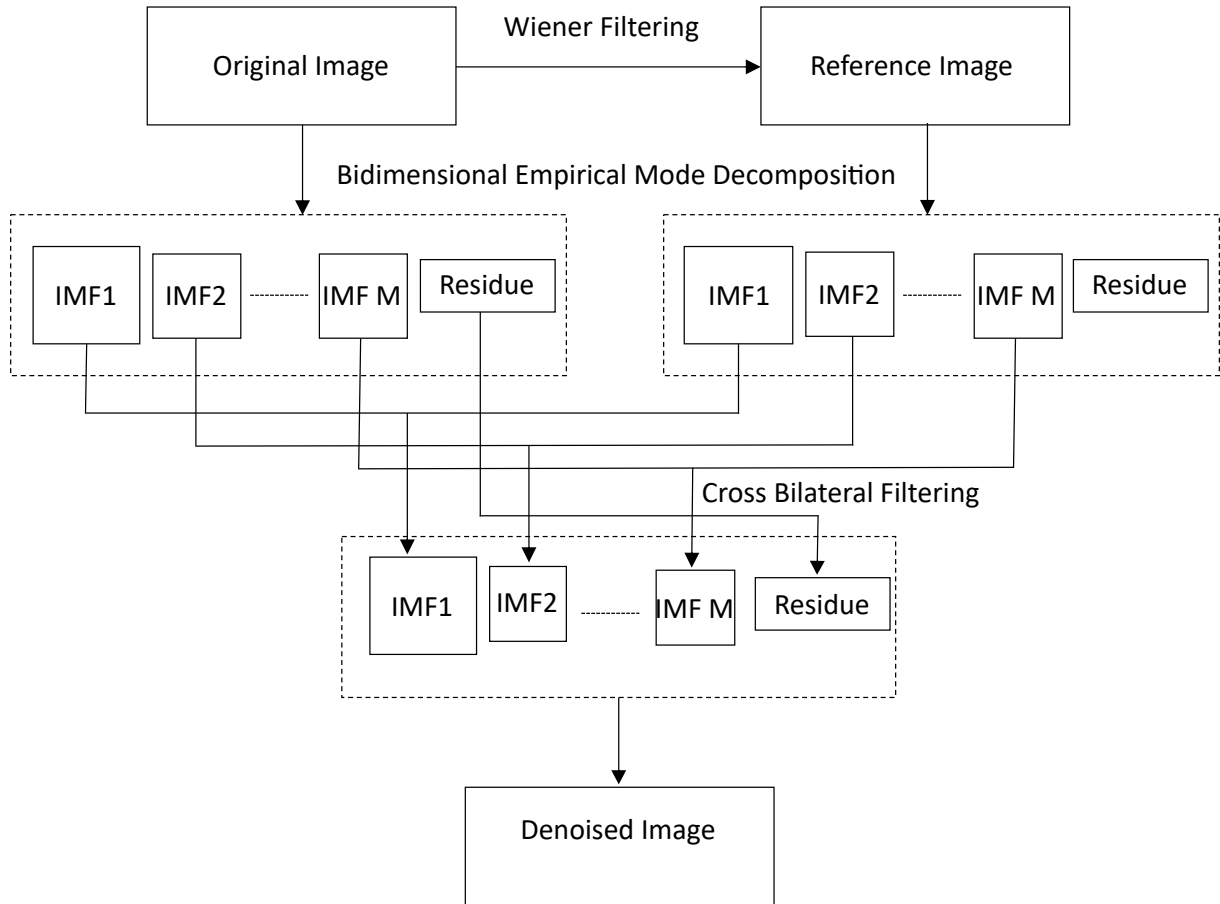


Fig. 1: Block Diagram of the proposed scheme.

dominant edge information as noise component has been reduced priorly. Also, the high order IMFs will have the smooth region information after the reduction of noise.

Hence, the proposed technique utilizes the dominant edge information in the low order IMFs of filtered image and the noise free non-edge information in the high order IMFs of this reference image. The algorithm applies the CBF between the same level IMFs of the original image and the filtered image referred to as *reference* image. This helps in preserving the edge details while removing the speckle noise from the ultrasound image as well as reduces the blurring in the smooth regions. The block diagram of the proposed algorithm is as shown in Fig. 1.

The steps in the proposed algorithm are as follows:

1. Calculate the BEMD of the original ultrasound image  $o(x, y)$  which has speckle noise.
2. Denoise the original noisy image with pixel-wise Wiener filter [37] to calculate the reference image. The noise component has to be additive while applying this filter, so the multiplicative speckle noise is converted to additive noise  $\eta(n_1, n_2)$  applying log transformation. Assuming that  $\eta(n_1, n_2)$  is having zero mean and variance  $\sigma_\eta^2$ , Wiener filter estimates the local mean and variance around each pixel of the chosen IMF.
3. Calculate the BEMD of the reference image calculated in step 2.
4. Apply CBF on all the IMFs of the original image taking the corresponding filtered image IMFs as the reference component.
5. Reconstruct the image from the output IMFs obtained in step 4 to get the final denoised image.

$$\mu_e = \frac{1}{NK} \sum_{x,y \in w} o(x, y), \quad (12)$$

$$\sigma_e^2 = \frac{1}{NK} \sum_{x,y \in w} o^2(x, y) - \mu_e^2, \quad (13)$$

where  $w$  is the window corresponding to the  $N \times K$  neighborhood of each pixel in the IMF. This filter then creates a pixel-wise estimate given as:

$$o_e(x, y) = \mu_e + \frac{\sigma_e^2 - \sigma_\eta^2}{\sigma_e^2} (o(x, y) - \mu_e). \quad (14)$$

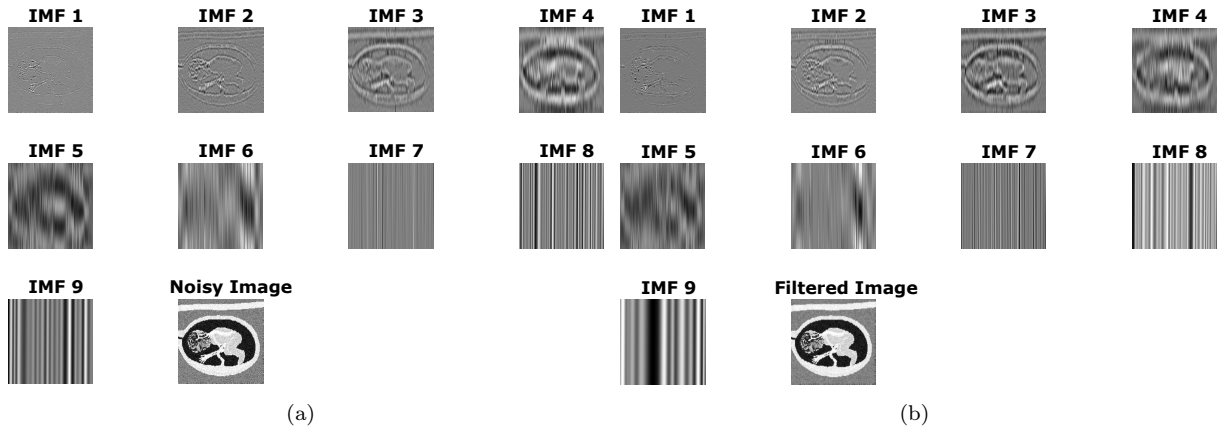


Fig. 2: (a) Noisy fetus image and its BEMD IMFs and (b) Filtered fetus image and its BEMD IMFs.

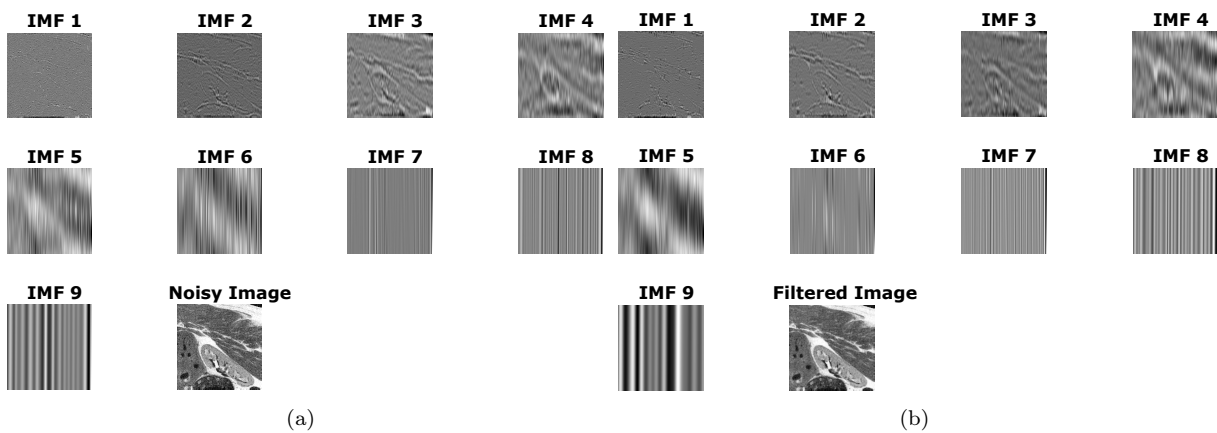


Fig. 3: (a) Noisy kidney image and its BEMD IMFs and (b) Filtered kidney image and its BEMD IMFs.

The pseudo code of the algorithm is as shown below:

- Read the noisy image  $I_n$  and resize it to a standard size as per the dataset:  $H_{size} = 256$ ;
- Calculate the IMFs of noisy image  $I_n$ :  
[imf, Res] = emd( $I_n$ );
- Wiener Filter the noisy image to obtain filtered image  $I_f$ :  
 $I_f = wiener2(I_n)$ ;
- Calculate the IMFs of filtered image:  
[imf2, Res2] = emd( $I_f$ );
- Modify IMFs using CBF taking distance sigma (sigmad), edge stopping sigma (sigmae), kernel size (ksize):  
For iteration  $i = 1 : size(imf,2)$ ;
  - Compute  $x(i) = imf(:,i)$ ;  
For iteration  $i = 1 : size(imf2,2)$ ;
  - Compute  $y(i) = imf2(:,i)$ ;  
For iteration  $i = 1 : size(x,2)$ ;
  - Calculate  $cbf\_out1(i) = cross\_bilateral\_filt(x(i), y(i), sigmad, sigmae, ksize)$ ;  
and  $detail1(i) = x(i) - cbf\_out1(i)$ ;
- Reconstruct the image:  
Recover = 0;  
Recover1 = 0;  
For iteration  $i = 1 : size(cb\_out1,2)$ ;
  - Calculate  $Recover1 = Recover1 + cbf\_out1(:,i) + detail1(:,i)$ ;  
 $Recover = Recover1 + Res$ ;

## 4. Experimental Results

The kidney and fetus synthetic images obtained using Field II simulation program [38] have been used in our experiments that were performed on MATLAB. The speckle noise has been added to the image with  $\sigma^2 = 0.1, 0.2, \text{ and } 0.3$ .

BEMD algorithm is applied on the noisy synthetic fetus image to obtain the IMFs and the residue.

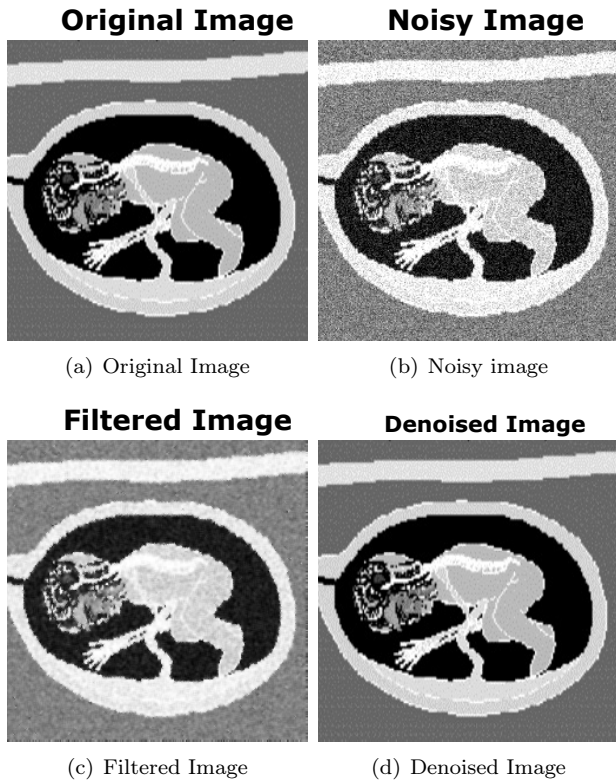


Fig. 4: Synthetic fetus image for  $\sigma^2 = 0.1$ .

Figure 2(a) shows the BEMD IMFs for noisy synthetic fetus image, that are obtained for noise variance  $\sigma^2 = 0.1$ . The spline interpolation that is used in our case is a cubic spline. The low order IMFs can be seen to have high frequency components corresponding to noise and edges of the image. As the Wiener filter gives optimal performance for additive noise, the multiplicative speckle was converted to additive noise using log-transformation before adding to the synthetic image.

Pixel-wise Wiener filtering utilizing 8-neighborhood for local region calculation was applied to the noisy image. The BEMD algorithm was then applied on this filtered image to get the IMFs which are shown in Fig. 2(b) along with residual image. It can be noted that the low order IMFs of the filtered image are now representing the dominant edge details.

As the Wiener filter has denoised the image, so IMFs of this filtered image are taken as the reference. CBF on all the IMFs of the noisy image and the corresponding IMFs of the filtered image has been applied to get the modified IMFs. Based on extensive experiments performed on different images, the value of distance sigma  $\sigma_d$ , edge stopping sigma  $\sigma_e$  and kernel size are undertaken as 1.8, 2.5, and 5, respectively for best results. These modified IMFs along with the residue of the input image are utilized to reconstruct the denoised image in which the edge information has been retained.

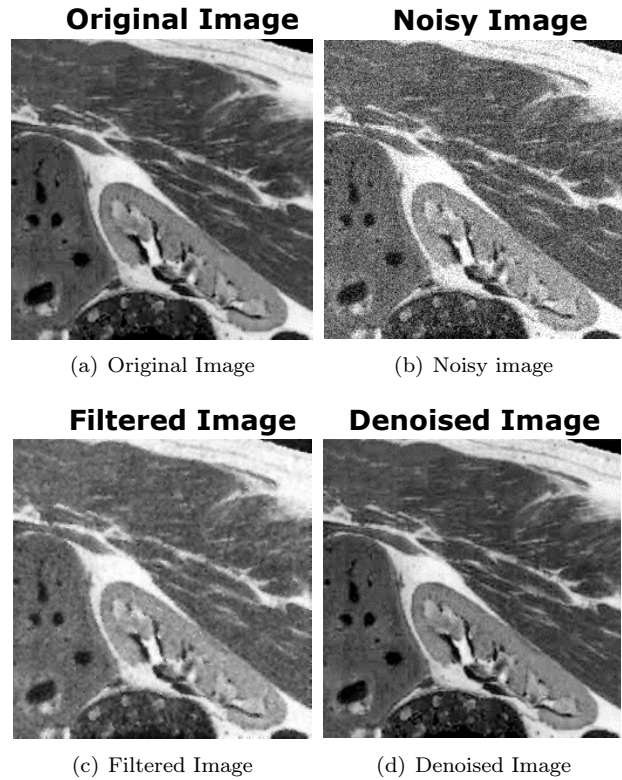
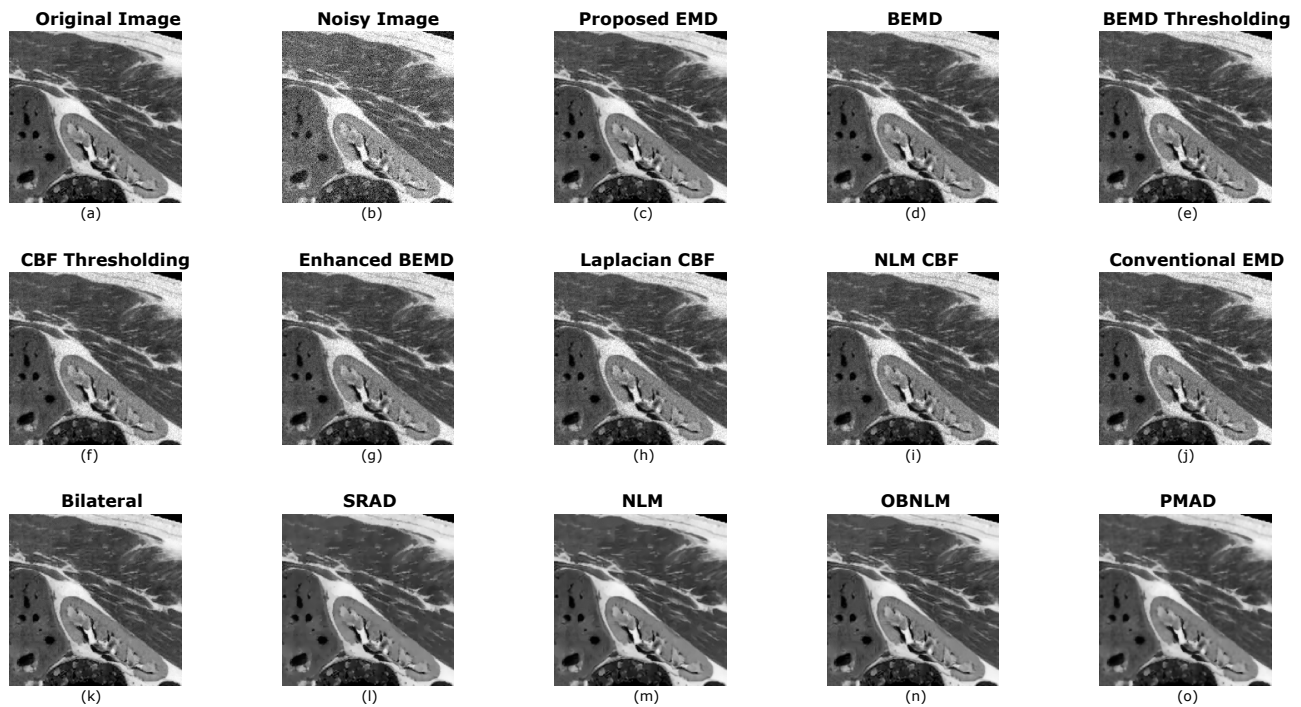


Fig. 5: Synthetic kidney image for  $\sigma^2 = 0.1$ .

Figure 4 shows the synthetic fetus image, its noisy version for  $\sigma^2 = 0.1$ , filtered reference image and the final reconstructed denoised image. As can be seen, the denoised image is perceptually of the same quality as that of the original image. Following the similar procedure results for the synthetic kidney image are obtained which are shown in Fig. 3 and Fig. 5, respectively. It is worth noting that the results provided by the proposed technique are perceptually very pleasing.

Table 2, Tab. 3, Tab. 4, Tab. 5, Tab. 6 and Tab. 7 shows the comparison of various parameters obtained for varying values of  $\sigma$  for the two Field II synthetic images, fetus and kidney. As can be noticed, the proposed algorithm performs better than the existing techniques in terms of EKI and PSNR, for noise variance  $\sigma^2 = 0.1, 0.2$  and  $0.3$ . The values obtained for EKI parameter gives better results even at higher noise variances, clearly showing better edge keeping capability of the proposed algorithm.

Also, as seen in the result tables, proposed technique gives comparable results with the existing techniques in terms of SNR, CC, SSIM and FOM for  $\sigma^2 = 0.1$ . At the same time, as can be analyzed from the values obtained by experimentation that the scheme is giving comparable results in terms of these parameters for higher values of  $\sigma^2 = 0.2$  and  $\sigma^2 = 0.3$  also. Thus, we can summarize that the technique performs acceptably well even at higher noise levels.



**Fig. 6:** Synthetic kidney: (a) Original image, (b) Noisy image for  $\sigma^2 = 0.1$ , Denoised images using the methods, (c) Proposed EMD technique, (d) BEMD [31], (e) BEMD Thresholding [32], (f) CBF Thresholding [36], (g) Enhanced BEMD [33], (h) Laplacian CBF [34], (i) NLM CBF [35], (j) Conventional EMD [30], (k) Bilateral [9], (l) SRAD [5], (m) NLM [11], (n) OBNLM [16] and (o) PMAD [7].

**Tab. 1:** Structural Similarity (SSIM) for various techniques.

Technique	MVR	ENL
Proposed technique	$18.81 \pm 2.63$	$5.41 \pm 2.37$
BEMD [31]	$18.51 \pm 3.76$	$5.25 \pm 2.79$
BEMD thresholding [32]	$18.13 \pm 4.02$	$5.18 \pm 2.82$
CBF thresholding [36]	$17.89 \pm 4.54$	$5.23 \pm 2.33$
Enhanced BEMD [33]	$18.02 \pm 4.93$	$5.14 \pm 2.64$
Laplacian CBF [34]	$17.95 \pm 4.82$	$5.11 \pm 2.18$
NLM CBF [35]	$17.63 \pm 4.22$	$5.01 \pm 2.13$
Conventional EMD [30]	$17.91 \pm 5.32$	$5.01 \pm 2.54$
Bilateral [9]	$15.42 \pm 5.16$	$3.96 \pm 2.32$
SRAD [5]	$17.66 \pm 4.52$	$4.87 \pm 2.35$
NLM [11]	$17.01 \pm 4.14$	$4.91 \pm 2.15$
OBNLM [16]	$17.81 \pm 4.71$	$4.95 \pm 2.61$
PMAD [7]	$16.39 \pm 6.21$	$4.33 \pm 2.79$

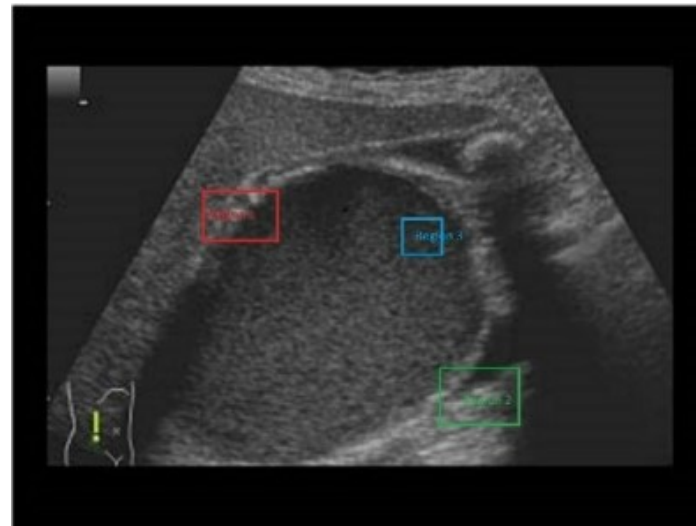
Figure 6 shows the visual results obtained by various denoising algorithms applied on the kidney image corrupted by a speckle of variance 0.1. It is clearly visible that the proposed technique is able to control the over smoothness shortcoming of some algorithms and also has better perceptual quality in terms of the edges in the image.

For the sake of completeness, the efficacy of proposed technique is also evaluated by performing experiments on the real ultrasound image database taken from [39]. The real images have three sets of data namely kidney, liver, and gall bladder images, each having around 85 images. Three regions were selected randomly for all three sets and the MVR and ENL have been calcu-

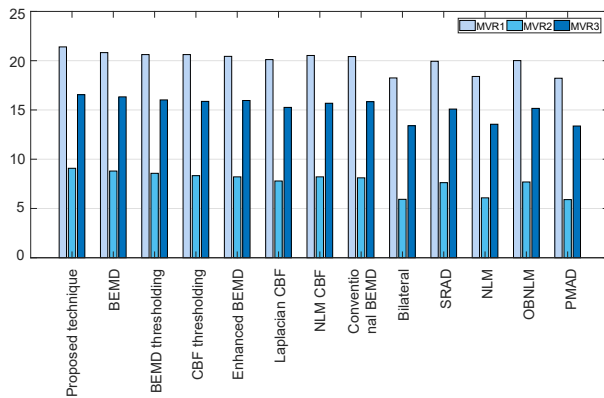
lated. The Fig. 7(a) shows the real liver ultrasound image, where three randomly selected regions are marked which are used for the calculation of MVR and ENL values. The Fig. 7(b) and Fig. 7(c) depicts the MVR and ENL plots obtained for selected regions in the real liver image database for comparing the performance of our proposed method with that of existing one. It is worth noting that our proposed method works fairly well compared to the others.

Table 1 shows the MVR and ENL mean values along with the standard deviation for the real liver ultrasound image database. Two different regions were selected in each US image for MVR and ENL calculation. These regions were randomly selected mainly in homogeneous and edge regions of a particular US image. Reconstructed US images were obtained for all the filters and MVR and ENL values were calculated in these regions. It is to be noted that the best MVR and ENL values are obtained for the proposed filter. Based on the results, the next candidate in terms of the performance was Laplacian CBF compared to the existing methods in terms of MVR and ENL values.

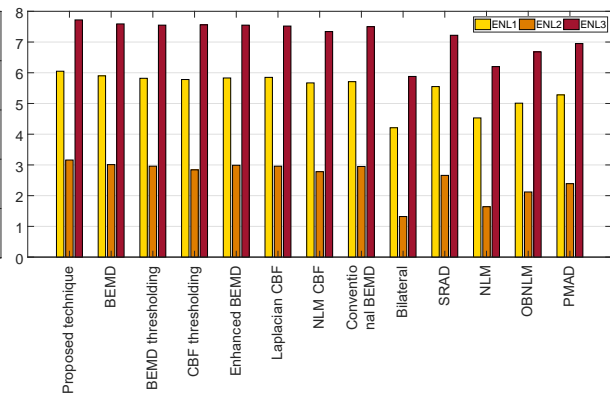
Similar experiments were performed on kidney and gall bladder real ultrasound image data sets also, however, due to paucity of space we have shown MVR and ENL plots for liver database only. The results obtained for the other sets are also in conjunction with the results shown here.



(a)



(b)



(c)

**Fig. 7:** (a) Real liver image with selected regions, (b) MVR plot and (c) ENL plot.

**Tab. 2:** Correlation Coefficient (CC) for various techniques.

Technique	CC					
	Noise variance $\sigma^2$					
	Synthetic fetus image			Synthetic kidney image		
	0.1	0.2	0.3	0.1	0.2	0.3
Proposed technique	0.95342	<b>0.93070</b>	<b>0.92330</b>	0.93840	<b>0.92590</b>	<b>0.88210</b>
BEMD [31]	<b>0.95834</b>	0.93007	0.92193	<b>0.94284</b>	0.90968	0.87969
BEMD thresholding [32]	0.95038	0.92852	0.91310	0.92435	0.88928	0.82736
CBF thresholding [36]	0.94911	0.90321	0.88398	0.91329	0.82987	0.77120
Enhanced BEMD [33]	0.95201	0.92654	0.87511	0.92643	0.88321	0.82101
Laplacian CBF [34]	0.93750	0.90440	0.89230	0.90760	0.85880	0.77830
NLM CBF [35]	0.94880	0.89530	0.87020	0.91020	0.83980	0.76430
Conventional EMD [30]	0.95102	0.92555	0.87480	0.92645	0.87332	0.81060
Bilateral [9]	0.91368	0.84291	0.78464	0.84947	0.74776	0.67000
SRAD [5]	0.94191	0.87916	0.81739	0.91540	0.82920	0.75551
NLM [11]	0.93126	0.87093	0.82044	0.87618	0.78484	0.71328
OBNLN [16]	0.95155	0.90697	0.86630	0.90923	0.83734	0.77571
PMAD [7]	0.94638	0.88481	0.82668	0.90595	0.80801	0.72333



**Tab. 3:** Signal to Noise Ratio (SNR) for various techniques.

Technique	SNR					
	Noise variance $\sigma^2$					
	Synthetic fetus image			Synthetic kidney image		
	0.1	0.2	0.3	0.1	0.2	0.3
Proposed technique	<b>14.0920</b>	12.8840	<b>11.4910</b>	15.5620	<b>13.9340</b>	12.4030
BEMD [31]	14.0620	12.6740	11.4590	<b>15.6020</b>	13.6940	<b>12.4430</b>
BEMD thresholding [32]	13.7653	12.1382	11.2891	15.1528	12.9726	12.0628
CBF thresholding [36]	12.7261	9.9268	8.2108	12.6753	11.4367	8.9624
Enhanced BEMD [33]	13.9211	11.2167	10.3427	14.4563	12.2731	10.3821
Laplacian CBF [34]	13.7400	<b>12.9200</b>	11.3230	14.5660	13.8250	12.3670
NLM CBF [35]	12.6540	9.8660	8.0320	12.4530	11.3450	8.0630
Conventional EMD [30]	13.9140	11.0110	10.2900	14.2440	12.0820	10.2030
Bilateral [9]	10.7200	7.9790	6.4897	10.7320	8.0182	6.5425
SRAD [5]	12.6000	9.2820	7.3429	13.7580	10.2860	8.4398
NLM [11]	11.7240	8.8585	7.3089	11.7650	8.9261	7.3852
OBNLM [16]	13.3050	10.3730	8.6871	13.3320	10.4920	8.8753
PMAD [7]	12.9410	9.4890	7.5779	13.2020	9.6131	7.6633

**Tab. 4:** Figure of Merit (FOM) for various techniques.

Technique	FOM					
	Noise variance $\sigma^2$					
	Synthetic fetus image			Synthetic kidney image		
	0.1	0.2	0.3	0.1	0.2	0.3
Proposed technique	0.88195	<b>0.85261</b>	<b>0.81317</b>	<b>0.88341</b>	0.85238	<b>0.83860</b>
BEMD [31]	0.82919	0.85146	0.81217	0.86334	<b>0.86088</b>	0.82560
BEMD thresholding [32]	0.81092	0.84838	0.80283	0.85392	0.84294	0.82934
CBF thresholding [36]	0.88392	0.82019	0.78291	0.85281	0.83827	0.77385
Enhanced BEMD [33]	0.83182	0.82791	0.79201	0.86389	0.83982	0.82739
Laplacian CBF [34]	0.88102	0.81890	0.77839	0.85930	0.83029	0.76321
NLM CBF [35]	0.88021	0.81820	0.77352	0.84920	0.82940	0.76429
Conventional EMD [30]	0.82761	0.84320	0.78133	0.86112	0.83281	0.81143
Bilateral [9]	0.81285	0.74764	0.70383	0.77549	0.72620	0.69278
SRAD [5]	0.86349	0.78487	0.73090	0.83815	0.75237	0.73401
NLM [11]	0.87531	0.79219	0.75194	0.83151	0.78397	0.74317
OBNLM [16]	<b>0.89364</b>	0.84390	0.80875	0.88295	0.78922	0.76806
PMAD [7]	0.86438	0.79341	0.73724	0.85802	0.76742	0.71880

**Tab. 5:** Peak Signal to Noise Ratio (PSNR) for various techniques.

Technique	PSNR					
	Noise variance $\sigma^2$					
	Synthetic fetus image			Synthetic kidney image		
	0.1	0.2	0.3	0.1	0.2	0.3
Proposed Technique	<b>24.983</b>	<b>23.117</b>	<b>22.748</b>	<b>24.821</b>	<b>22.281</b>	<b>21.842</b>
BEMD [31]	24.946	23.077	22.383	24.322	22.188	21.158
BEMD thresholding [32]	24.126	22.764	21.853	23.019	21.934	21.021
CBF thresholding [36]	24.421	21.839	22.210	23.583	21.021	21.012
Enhanced BEMD [33]	22.593	21.294	21.256	22.593	21.245	20.183
Laplacian CBF [34]	23.453	20.987	20.837	24.839	20.548	20.634
NLM CBF [35]	24.332	21.712	22.590	23.383	20.628	21.522
Conventional EMD [30]	22.398	20.671	20.330	22.317	20.672	19.821
Bilateral [9]	21.056	18.009	16.260	19.025	15.992	14.254
SRAD [5]	23.058	19.463	17.260	22.192	18.459	16.398
NLM [11]	22.336	19.310	17.594	20.288	17.239	15.518
OBNLM [16]	24.002	21.030	19.306	21.971	19.054	17.350
PMAD [7]	23.539	19.837	17.690	21.730	17.878	15.686

**Tab. 6:** Edge Keeping Index (EKI) for various techniques.

Technique	EKI					
	Noise variance $\sigma^2$					
	Synthetic fetus image			Synthetic kidney image		
	0.1	0.2	0.3	0.1	0.2	0.3
Proposed technique	<b>0.64911</b>	<b>0.60185</b>	<b>0.54098</b>	<b>0.55280</b>	<b>0.50382</b>	<b>0.49382</b>
BEMD [31]	0.64603	0.59358	0.53587	0.54885	0.50024	0.49063
BEMD thresholding [32]	0.63914	0.57292	0.52177	0.53922	0.48392	0.48392
CBF thresholding [36]	0.62797	0.56821	0.53676	0.53182	0.49910	0.47829
Enhanced BEMD [33]	0.62381	0.53725	0.51829	0.52003	0.49201	0.45729
Laplacian CBF [34]	0.63920	0.57492	0.52780	0.53720	0.50220	0.47399
NLM CBF [35]	0.62670	0.55930	0.52180	0.52180	0.50000	0.47290
Conventional EMD [30]	0.61720	0.52081	0.50012	0.51320	0.48230	0.45321
Bilateral [9]	0.59360	0.54006	0.52306	0.53703	0.49294	0.47574
SRAD [5]	0.55134	0.49815	0.49498	0.49201	0.45619	0.43757
NLM [11]	0.59768	0.54228	0.51775	0.53614	0.49024	0.47184
OBNL [16]	0.62562	0.54757	0.52198	0.55135	0.49023	0.46734
PMAD [7]	0.55606	0.50568	0.49567	0.49833	0.46407	0.44813

**Tab. 7:** Structural Similarity (SSIM) for various techniques.

Technique	SSIM					
	Noise variance $\sigma^2$					
	Synthetic fetus image			Synthetic kidney image		
	0.1	0.2	0.3	0.1	0.2	0.3
Proposed technique	<b>0.78918</b>	0.68291	<b>0.63330</b>	<b>0.62688</b>	0.53321	0.49197
BEMD [31]	0.70575	0.66684	0.62823	0.61088	<b>0.53961</b>	<b>0.49347</b>
BEMD thresholding [32]	0.68381	0.65382	0.61933	0.60012	0.48932	0.48293
CBF thresholding [36]	0.76290	0.65378	0.60832	0.61092	0.44103	0.38173
Enhanced BEMD [33]	0.73829	0.66362	0.62190	0.62811	0.50021	0.46738
Laplacian CBF [34]	0.74920	0.64920	0.53920	0.60372	0.49240	0.31733
NLM CBF [35]	0.75920	0.64938	0.59380	0.61930	0.43582	0.37290
Conventional EMD [30]	0.72345	0.65482	0.61291	0.61098	0.49308	0.45320
Bilateral [9]	0.71808	0.61478	0.55520	0.53328	0.39544	0.32945
SRAD [5]	0.76831	0.67000	0.59414	0.65411	0.50453	0.41941
NLM [11]	0.74678	0.64120	0.58082	0.56396	0.42391	0.35323
OBNL [16]	0.78688	<b>0.68623</b>	0.62356	0.62079	0.47589	0.39955
PMAD [7]	0.78014	0.68009	0.60847	0.63845	0.47608	0.38675

## 5. Conclusion

In this paper, a BEMD based cross bilateral filtering technique for US image denoising was presented. The proposed method solves the problem of losing the edge information in the conventional BEMD based denoising techniques. As the conventional BEMD based algorithm worked on the removal of low order IMFs, it was losing important edge information which has been preserved with the help of the proposed method. The performance of the method has been verified quantitatively in terms of PSNR, EKI, SSIM, FOM, SNR, and CC for synthetic ultrasound images. The quantitative analysis is also done on the real ultrasound images in terms of MVR and ENL. It has been found that the proposed algorithm performs better than many other existing states of art techniques and can preserve the edge information.

## Author Contributions

V.K. conceived the presented idea. B.G. developed the theory and performed the experiments. V.K. encouraged B.G. to investigate and supervised the findings of this work. Both authors discussed the results and contributed to the final manuscript.

## References

- [1] BURCKHARDT, C. B. Speckle in ultrasound B-mode scans. *IEEE Transactions on Sonics and Ultrasonics*. 1978, vol. 25, iss. 1, pp. 1–6. ISSN 2162-1403. DOI: 10.1109/T-SU.1978.30978.
- [2] SZABO, T. L. *Diagnostic Ultrasound Imaging: Inside Out..* 2nd ed. Boston: Academic Press,

2014. ISBN 97-801-2396-5424.
- [3] WANG, Z., A. BOVIK, H. SHEIKH and E. SIMONCELLI. Image quality assessment: from error visibility to structural similarity. *IEEE Transactions on Image Processing*. 2004, vol. 13, iss. 4, pp. 600–612. ISSN 1941-0042. DOI: 10.1109/TIP.2003.819861.
- [4] RODGERS, J. and W. A. NICEWANDER. Thirteen Ways to Look at the Correlation Coefficient. *The American Statistician*. 1988, vol. 42, iss. 1, pp. 59–66. ISSN 1537-2731. DOI: 10.1080/00031305.1988.10475524.
- [5] YU, Y. and S. ACTON. Speckle reducing anisotropic diffusion. *IEEE Transactions on Image Processing*. 2002, vol. 11, iss. 11, pp. 1260–1270. ISSN 1941-0042. DOI: 10.1109/TIP.2002.804276.
- [6] RAHIMI, M. and M. YAZDI. A new hybrid algorithm for speckle noise reduction of SAR images based on mean-median filter and SRAD method. In: *2nd International Conference on Pattern Recognition and Image Analysis (IPRIA)*. Rasht: IEEE, 2015, pp. 1–6. ISBN 978-1-4799-8445-9. DOI: 10.1109/PRIA.2015.7161623.
- [7] LIU, X., J. LIU, X. XU, L. CHUN, J. TANG and Y. DENG. A robust detail preserving anisotropic diffusion for speckle reduction in ultrasound images. *BMC Genomics*. 2011, vol. 12, iss. 5, pp. 1260–1270. ISSN 1471-2164. DOI: 10.1186/1471-2164-12-S5-S14.
- [8] PERONA, P. and J. MALIK. Scale-space and edge detection using anisotropic diffusion. *IEEE Transactions on Pattern Analysis and Machine Intelligence*. 1990, vol. 12, iss. 7, pp. 629–639. ISSN 1939-3539. DOI: 10.1109/34.56205.
- [9] TOMASI, C. and R. MANDUCHI. Bilateral filtering for gray and color images. In: *Sixth International Conference on Computer Vision*. Bombay: IEEE, 1998, pp. 839–846. ISBN 81-7319-221-9. DOI: 10.1109/ICCV.1998.710815.
- [10] BALOCCO, S., C. GATTA, O. PUJOL, J. MAURI and P. RADEVA. SRBF: Speckle reducing bilateral filtering. *Ultrasound in Medicine & Biology*. 2010, vol. 36, iss. 8, pp. 1353–1363. ISSN 0301-5629. DOI: 10.1016/j.ultrasmedbio.2010.05.007.
- [11] PIERRICK, C., H. PIERRE, K. CHARLES and B. CHRISTIAN. Nonlocal means-based speckle filtering for ultrasound images. *IEEE Transactions on Image Processing*. 2009, vol. 18, iss. 10, pp. 2221–2229. ISSN 1941-0042. DOI: 10.1109/TIP.2009.2024064.
- [12] Yi, Z., M. DING, L. WU and X. ZHANG. Non-local means method using weight refining for despeckling of ultrasound images. *Signal Processing*. 2014, vol. 103, iss. C, pp. 201–213. ISSN 0165-1684. DOI: 10.1016/j.sigpro.2013.12.019.
- [13] LI, X., H. HE, R. WANG and J. CHEN. Superpixel-guided nonlocal means for image denoising and super-resolution. *Signal Processing*. 2016, vol. 124, iss. C, pp. 173–183. ISSN 0165-1684. DOI: 10.1016/j.sigpro.2015.09.021.
- [14] GUO, Y., Y. WANG and T. HOU. Superpixel-guided nonlocal means for image denoising and super-resolution. *Biomedical Signal Processing and Control*. 2011, vol. 6, iss. 2, pp. 129–138. ISSN 1746-8094. DOI: 10.1016/j.bspc.2010.10.004.
- [15] KERVRANN, C., J. BOULANGER and P. COUPE. Bayesian Non-local Means Filter, Image Redundancy and Adaptive Dictionaries for Noise Removal. In: *International Conference on Scale Space and Variational Methods in Computer Vision (SSVM)*. Ischia: Springer, 2007, pp. 520–532. ISBN 978-3-540-72823-8. DOI: 10.1007/978-3-540-72823-8\_45.
- [16] COUPE, P., P. HELLIER, C. KERVRANN and C. BARILLOT. Bayesian non local means-based speckle filtering. In: *5th IEEE International Symposium on Biomedical Imaging: From Nano to Macro*. Paris: IEEE, 2008, pp. 1291–1294. ISBN 978-1-4244-2002-5. DOI: 10.1109/ISBI.2008.4541240.
- [17] YANG, J., J. FAN, D. AI, X. WANG, Y. ZHENG, S. TANG and Y. WANG. Local statistics and non-local mean filter for speckle noise reduction in medical ultrasound image. *Neurocomputing*. 2016, vol. 195, iss. 1, pp. 88–95. ISSN 0925-2312. DOI: 10.1016/j.neucom.2015.05.140.
- [18] MEI, F., D. ZHANG and Y. YANG. Improved non-local self-similarity measures for effective speckle noise reduction in ultrasound images. *Computer Methods and Programs in Biomedicine*. 2020, vol. 196, iss. 1, pp. 1–14. ISSN 0169-2607. DOI: 10.1016/j.cmpb.2020.105670.
- [19] HUANG, S., C. TANG, M. XU, Y. QIU and Z. LEI. BM3D-based total variation algorithm for speckle removal with structure-preserving in OCT images. *Applied Optics*. 2019, vol. 58, iss. 23, pp. 6233–6243. ISSN 1559-128X. DOI: 10.1364/AO.58.006233.
- [20] CAI, C., M. DING and C. ZHOU. Bilateral filtering in the wavelet domain. In: *Multispectral Image Processing and Pattern Recognition: Image Matching and Analysis*. Wuhan:

- SPIE, 2001, pp. 246–252. ISBN 981-02-4593-9. DOI: 10.1117/12.441517.
- [21] EISEMANN, E. and F. DURAND. Flash photography enhancement via intrinsic relighting. *ACM Transactions on Graphics*. 2004, vol. 23, iss. 3, pp. 673–678. ISSN 1557-7368. DOI: 10.1145/1015706.1015778.
- [22] DURAND, F. and J. DORSEY. Fast Bilateral Filtering for the Display of High-Dynamic-Range Images. *ACM Transactions on Graphics*. 2002, vol. 21, iss. 3, pp. 257–266. ISSN 1557-7368. DOI: 10.1145/566654.566574.
- [23] PHAM, T. Q. and L. J. VLIET. Separable bilateral filtering for fast video preprocessing. In: *IEEE International Conference on Multimedia and Expo*. Amsterdam: IEEE, 2005, pp. 1–4. ISBN 0-7803-9331-7. DOI: 10.1109/ICME.2005.1521458.
- [24] PARIS, S. and F. DURAND. A Fast Approximation of the Bilateral Filter Using a Signal Processing Approach. *International Journal of Computer Vision*. 2009, vol. 81, iss. 1, pp. 24–52. ISSN 1573-1405. DOI: 10.1007/s11263-007-0110-8.
- [25] GEORG, P., R. SZELISKI, M. AGRAWALA, M. COHEN, H. HOPPE and K. TOYAMA. Digital photography with flash and no-flash image pairs. *ACM Transactions on Graphics*. 2004, vol. 23, iss. 3, pp. 664–672. ISSN 1557-7368. DOI: 10.1145/1015706.1015777.
- [26] HUANG, N. E., Z. SHEN, S.R. LONG, M. C. WU, H. H. SHIH, Q. ZHENG, N.-C. YEN, C. C. TUNG and H. H. LIU. The empirical mode decomposition and the Hilbert spectrum for nonlinear and non-stationary time series analysis. *The Royal Society Publishing*. 1998, vol. 454, iss. 1971, pp. 903–998. ISSN 1471-2946. DOI: 10.1098/rspa.1998.0193.
- [27] LINDERHED, A. Image Empirical Mode Decomposition: a New Tool for Image Processing. *Advances in Adaptive Data Analysis*. 2009, vol. 1, iss. 2, pp. 265–294. ISSN 1793-7175. DOI: 10.1142/S1793536909000138.
- [28] KOPSINIS, Y. and S. MCLAUGHLIN. Development of EMD-Based Denoising Methods Inspired by Wavelet Thresholding. *IEEE Transactions on Signal Processing*. 2009, vol. 57, iss. 4, pp. 1351–1362. ISSN 1941-0476. DOI: 10.1109/TSP.2009.2013885.
- [29] NUNES, J. C., Y. BOUAOUNE, E. DELECELLE, O. NIANG and P. BUNEL. Image analysis by bidimensional empirical mode decomposition. *Image and Vision Computing*. 2003, vol. 21, iss. 12, pp. 1019–1026. ISSN 1941-0476. DOI: 10.1016/S0262-8856(03)00094-5.
- [30] NUNES, J. C., S. GUYOT and E. DELECELLE. Texture analysis based on Bidimensional Empirical Mode Decomposition and quaternions. *Machine Vision and Applications*. 2005, vol. 16, iss. 3, pp. 177–188. ISSN 1432-1769. DOI: 10.1007/s00138-004-0170-5.
- [31] GUPTA, B. and V. KHANDELWAL. BEMD Based Ultrasound Image Speckle Reduction Technique Using Pixel-Wise Wiener Filtering. *Advances in Electrical and Electronic Engineering*. 2021, vol. 19, iss. 2, pp. 168–178. ISSN 1804-3119. DOI: 10.15598/aeec.v19i2.4100.
- [32] LIU, D. and X. CHEN. Image denoising based on improved bidimensional empirical mode decomposition thresholding technology. *Multimedia Tools and Applications*. 2019, vol. 78, iss. 1, pp. 7381–7417. ISSN 1380-7501. DOI: 10.1007/s11042-018-6503-6.
- [33] AN, F., D. LIN, X. ZHOU and Z. SUN. Enhancing Image Denoising Performance of Bidimensional Empirical Mode Decomposition by Improving the Edge Effect. *International Journal of Antennas and Propagation*. 2015, vol. 2015, iss. 1, pp. 1–12. ISSN 1687-5877. DOI: 10.1155/2015/769478.
- [34] MENG, W., Z. HUIHENG and H. HE. A Pseudo Cross Bilateral Filter for Image Denoising Based on Laplacian Pyramid. In: *IEEE International Symposium on Knowledge Acquisition and Modeling Workshop*. Wuhan: IEEE, 2008, pp. 1–4. ISBN 978-1-4244-3530-2. DOI: 10.1109/KAMW.2008.4810469.
- [35] FENG, W.-Q., S. M. LI and K.-L. ZHENG. A non-local bilateral filter for image denoising. In: *International Conference on Apperceiving Computing and Intelligence Analysis Proceeding (ICACIA)*. Chengdu: IEEE, 2010, pp. 253–257. ISBN 978-1-4244-8026-5. DOI: 10.1109/ICACIA.2010.5709895.
- [36] YAMAGUCHI, T. and M. IKEHARA. Joint bilateral based image denoising using multi-sized 2D hard threshold. In: *Asia-Pacific Signal and Information Processing Association Annual Summit and Conference (APSIPA ASC)*. Kuala Lumpur: IEEE, 2017, pp. 1178–1181. ISBN 978-1-5386-1542-3. DOI: 10.1109/APSIPA.2017.8282207.
- [37] LIM, J. S. *Two-Dimensional Signal and Image Processing*. 1st ed. Upper Saddle River: Prentice Hall PTR, 1990. ISBN 978-0-13-935322-2.
- [38] JENSEN, A. J. A Program for Simulating Ultrasound Systems. *Medical & Biological Engineering & Computing*. 1996, vol. 34, iss. 1, pp. 351–353. ISSN 1741-0444.

[39] Image Database: *Ultrasound cases* [online]. Available at: <http://www.ultrasoundcases.info>.

## About Authors

**Bhawna GUPTA** (corresponding author) joined the Department of Electronics and Communication Engineering, Jaypee Institute of Information Technology, Noida, in 2003 and is currently working as Assistant Professor. She received her B.Tech and M.Tech degree from Aligarh Muslim University (AMU), Aligarh, India. She is currently pursuing Ph.D. from Jaypee Institute of Information Technology, Noida, India in

the area of image processing. Her research interests include biomedical signal processing and digital signal processing.

**Vineet KHANDELWAL** is working as Associate Professor at the Department of Electronics and Communication Engineering, Jaypee Institute of Information Technology, Noida. He received his Ph.D degree from School of Computer Systems and Sciences, JNU, New Delhi, India and M.Tech in Signal Processing from NSIT, New Delhi, India. He obtained his B.E degree in Electronics and Communication Engineering from MITS, Gwalior. His research interests include signal processing, biomedical signal processing and RF & Optical wireless communication etc.